Calculation of Torque Generation in Bacterial Flagellar Motor

A.Akashnathan
IIT Madras, *bs16b031@smail.iitm.ac.in*

Adviser: Prof. Manoj Varma
CENSE,IISc, *mvarma@iisc.ac.in*

July 2019

ABSTRACT

The locomotion of a Bacteria is assisted by the Flagella. These flagella act as a propeller with the help of a tiny rotary motor of diameter 45nm. These rotors generate torque in the order of 150pNnm. These generate a unique and interesting Torque vs speed curves. This still remains one of the fundamental problems in Biophysics and so many hypothetical models have come up since the 1970s. A recent study on single stator motor has revealed a concave down curve for the Torque vs speed plot. Using this and many other experimental data including some key concepts from some theoretical models proposed since the 1970s, K.K Mandadapu has created a mechanochemical model[6]. This model is the first model to explain the torque generation physically, instead of using the energy equation as before[14]. This model as of now explains most of the questions raised regarding the torque generation. This report is about the study on this mechanochemical model, calculating Torque and implementation of this model. The knee region calculation is also explained in this report.

Keywords: BFM - Bacterial Flagellar Motor, PMF- Proton Motive Force, SMF- Sodium ion Motive Force, T_m- moving time, T_w- waiting time, SDE- Stochastic Differential Equation, ODE- Ordinary Differential Equation

1 INTRODUCTION

The torque generation of the BFM still remains a mystery due to the lack of technology to actually see the motor. Many studies are done on the BFM and each one gives a result which makes the overall interpretation difficult[9][13]. These motors, unlike the other Biological motors, run on the PMF or IMF(Ion Motive Force), confirmed by an experiment on a starving bacteria in 1977[7],

$$IMF = V_m + \frac{k_B T}{q} \log \frac{C_i}{C_o}.$$

Many new techniques have been used to experimentally calculate the torque generation. Two major experiments are done for the study of Torque Vs Speed curve
First, the initial experiment used to calculate the torque is by tethering the cell so that

the cell body acts as load and slows down the rotation making it visible to the human eyes under microscope[12]. Later Bead Assay started taking place[1], in which a load(ζ_L) is attached to the flagella and the movement is noted. The torque and speed relation would be $\tau_M = (\zeta_L + \zeta_R)\omega \approx \zeta_L\omega$.
Second, then people started generating external torque to the tethered cell[2]. The torque ad speed relationship now would be $\tau_{ext} + \tau_M = (\zeta_L + \zeta_M)\omega$. Now the torque direction is reversed so that the motor is broken and the speed is only due to the external torque. Hence the motor torque is calculated by $\tau_M = (\zeta_M + \zeta_L)(\omega - \omega')$, where ω' is the speed of motor purely due to the τ_{ext}.

After giving some insights about the experimental calculation let me give you the major problems faced and the characteristic nature of the Torque vs speed curve. The major problem faced after the resurrection experiments[11] are the zero load Torque generation[15], where the motor in a single activation produced maximum speed generation. After this recently another experiment revealed that the number of stators getting activated depends on the the load attached to it[4]. This made the interpretation of the zero torque speed even more difficult as now we cant say how many stators were activated while producing the zero torque. Imaging of torque generation in BFM still remains a challenge. So, people started giving some hypothetical models[9]. The characteristic nature of the BFM is given in figure1.

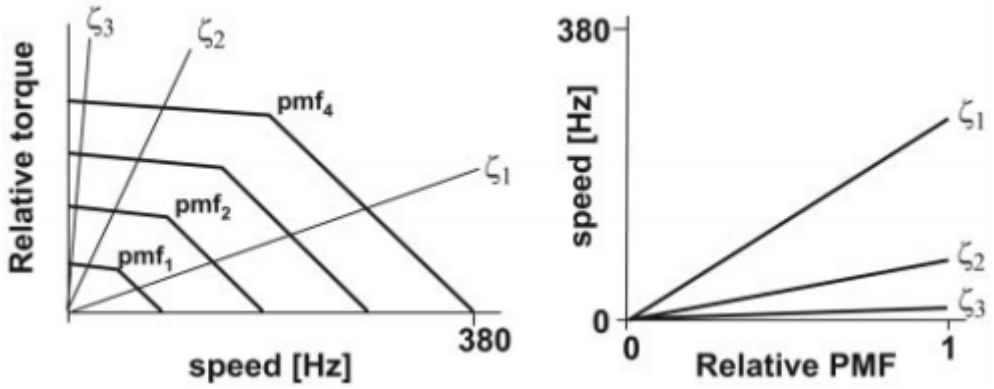

Figure 1: Chactaristic plots of the BFM[14]

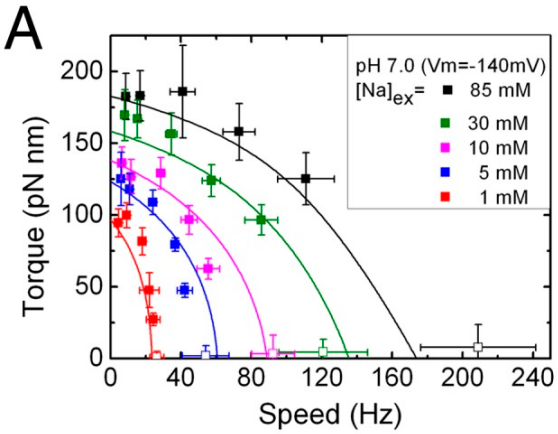

Figure 2: Torque speed characteristics of single stator motor[5].

Recent study on single stator motor[5] has revealed a different kind of curve. Instead for showing a knee speed point it was a concave down curve as in figure2

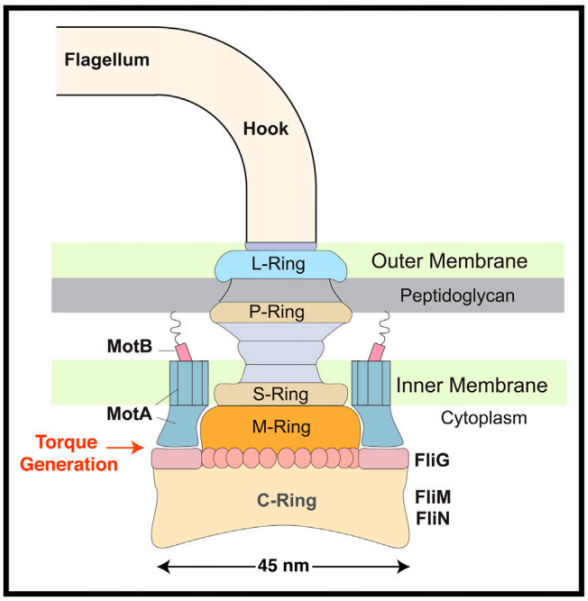

Figure 3: Structure of BFM [9]

Now, before going to the model let us discuss about the BFM structure we know. So as shown in figure3 the rings of the basal body of the BFM acts as a rotor. The FliG is the primary component of the rotor in torque generation. The MotA and MotB complex acts as the stator . The molecular formula from stoichiometry is A_4B_2 , meaning a single stator contains 4 MotA loops and 2 MotB loops. Given these information let's move on to the Model and the implementation parts[13].

2 MODEL

The Mandadapu's model for a single stator torque generation is a mechanochemical model[6], meaning it involves both the mechanical properties and the chemical properties like dissociation constant(K_d), concentration of the particular ion, etc. The figure 4 is the pictorial representation of the model. In molecular level, the model revolves around two convered residues Pro173 of MotA and Asp32 of MotB (as seen in figure 5).

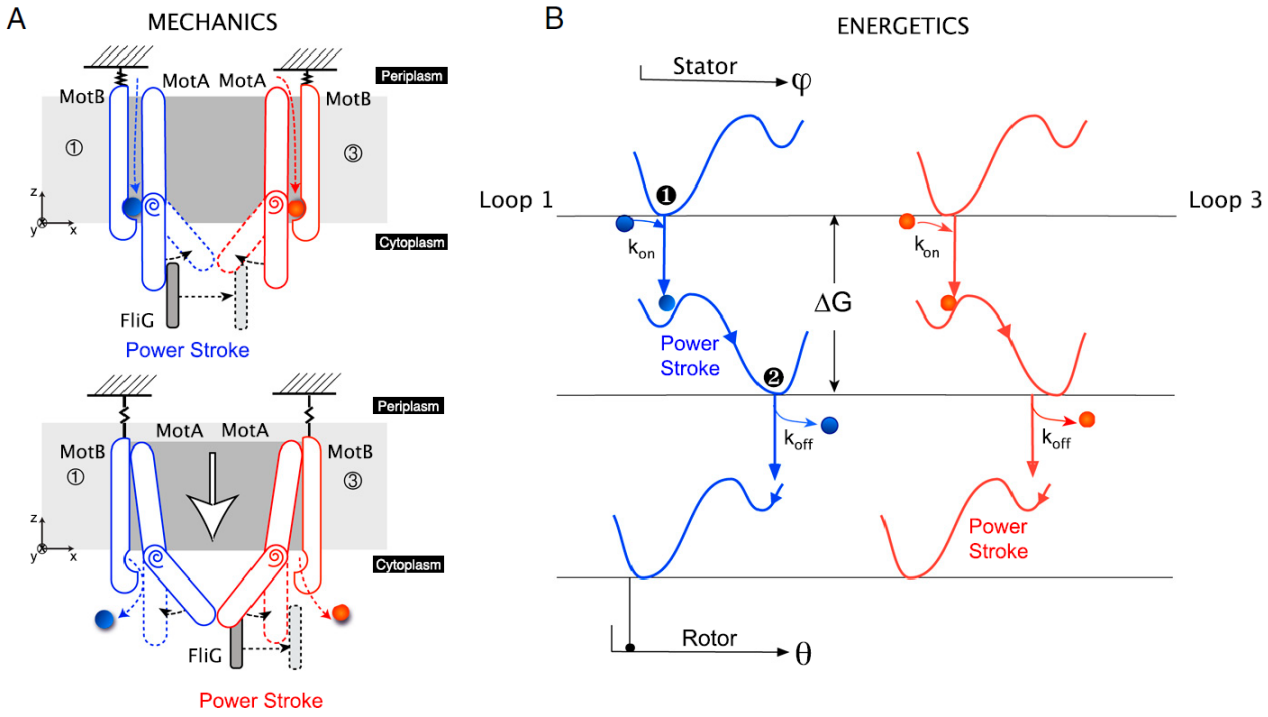

Figure 4: Mandadapu's model for single stator[6]

The model involves two phenomenon Electrostatic/chemical and the Steric potential. The electrostatic makes the loops to stay in the nearest place to the FliG loops and the Chemical phenomenon involves the ion binding step . The time involved during this is called the T_w (waiting Time). Now the steric potential is the one which delivers the torque as the MotA loops hit the FliG loop. This model is similar to the 2 cylinder car engine model. It is arbitrarily considered that the loops 1 and 3 involve in rotating the flagella in one particular direction and the 2 and 4 loop involve in the other direction. The time taken for this mechanical pus is called T_m (moving Time).Note that the motor is in low Reynolds Number[10] regime , hence once the pushing stops the motor stops moving as the viscous factor is more

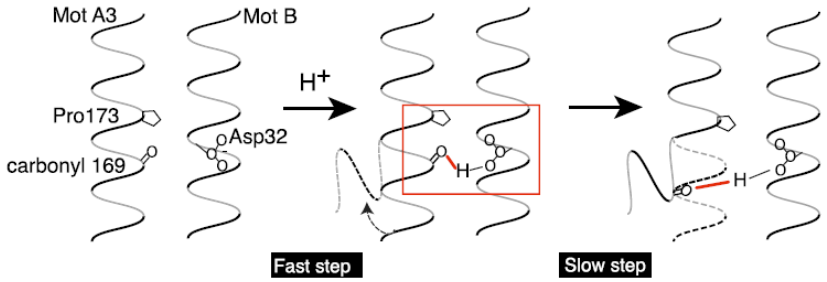

Figure 5: Molecular level understanding of the rotation about the Pro173 residue in MotA loop[6]

A single step in this model involes two power stroke and from the experimental data each step of the motor involves a rotation of the rotor (FliG) about $\frac{2\pi}{26}$(0.241661 rads). The bending in the stator is denoted by ϕ and the rotation in rotor is denoted by θ_L and the

rotation of the load is denoted by θ_L. The stator can move up to 20° for a particular power stroke (0.3491 rads).

The steps involved in moving a rotor for $\frac{2\pi}{26}$, that is , for a single step rotation of single stator is given below:

- The ion from the periplasm binds to the Asp32 of MotB and as soon as the binding takes place there is a conformation change in the stator.
- Now the confirmation change involves a rotation of motA about the Pro173 and a downward motion of the whole stator.
- During this movement, first Power stroke is delivered by the MotA loop 1.
- Due to this there is a rotation in the rotor . Now due to the vertical motion the ion is exposed to the cytoplasm and hence the ion dissociates into the cytoplasm
- As soon as the ion goes into the cytoplasm confirmation of the stator goes back to the initial structure.
- Due to this the 3rd loop delivers the second Power stroke.

This model describes the curves of the Torque vs speed graph is due to the T_m and T_w. This statement is discussed in the Discussion section .

Parameters involved:

θ_R- angle made during the rotor's rotation
ϕ_S- angle made during the stator's rotation
θ_L-angle made during the load's rotation
Time derivatives of these angles denote their corresponding angular speed ζ_L- drag co-efficient of load
ζ_R- drag co-efficient of rotor
ζ_S- drag co-efficient of stator
l_p- distance from the Pro173 to the cytoplasmic end of the MotA loop
R- radius of the rotor
F_p- The force along the tangential direction of the stator about Pro173 ($= |\frac{1}{l_p}\frac{\partial G}{\partial \phi_S}|$)
k- The torsional restoration force constant from the hook
ψ- The electrical potential due to interaction between stator and rotor only.

3 METHODS

The model is written as 3 Langevin equation. Hence for the implementation of the model numerical simulation of these 3 Langevin equation is important.

$$\zeta_S \frac{d\phi_S}{dt} = -\frac{\partial G(\phi_S, j)}{\phi_S} - \frac{\partial V_{RS}}{\partial \phi_S} - \frac{\partial \psi}{\partial \phi_S} + \sqrt{2k_B T \zeta_S} f_n(t) \tag{1}$$

$$\zeta_R \frac{d\theta_R}{dt} = -\frac{\partial V_{RS}}{\partial \theta_R} - \frac{\partial \psi}{\partial \theta_R} - k(\theta_R - \theta_L) + \sqrt{2k_B T \zeta_R} f_n(t) \tag{2}$$

$$\zeta_L \frac{d\theta_L}{dt} = k(\theta_R - \theta_L) + \sqrt{2k_B T \zeta_L} f_n(t) \tag{3}$$

Equation 1 is for the dynamics of the stator where the first term is the torque due to conformation change, the second term is the torque due to the steric push and the third term is due to the electrostatic potential. In equation 2 , which is for rotor, the term with k is due to the torsional restoration force from the hook hence there is a restoring torque. The equation is self explanatory . All these equations involves a term for Thermal fluctuation. Hence it is a SDE. SDE numerical simulation has to be done.

For the implementation of this model:

- First we begun with solving analytically the deterministic form of the equation to see the curve nature. But the equation were bulky and complex with lot of parameters. Some of the analytical solution is there in the APPENDIX.
- Next, we did numerical simulation for the deterministic form to see the nature of the curve.This was done using ODE23,ODE45,Euler method for comparison study .By implementing Euler it is easy to do some changes and implement the Euler Maruyama method for SDE[3].
- During the numerical simulation first challenge was T_m calculation. This we did by following its definition of moving a FliG loop by $\frac{2\pi}{26}$.
- second challenge faced by us was T_w calculation, but this remained unresolved as of now as the kinetic model for the ion hopping were done for $[H^+]$ ion. To get the numerical value from this model some of the experimental data were required and random numbers cannot be inputted as there were many parameters. Hence, we took an average T_w value specified in the Mandadapu's paper.
- Now the curves were generated for the deterministic model by calculating average Torque during a single step over different loads.

$$\tau_{avg} = \frac{1}{T}\int_0^T \tau_{inst} dt \approx \frac{\sum_{i=0}^{n} \tau_i \Delta t}{T_m + T_w}$$

  Where $t_n = T_m$, this is because during T_w there is no torque[10][8] or ω_R. Similarly, $\omega_{R_{avg}}$ can be calculated in the same way by numerically.
- Now for the SDE Euler Maruyama method is used where the Brownian motion part is sum-mated with time step $= \sqrt{dt}$. Explanation is given in the APPENDIX. Curves is shown in the Results.
- During this a condition was for the knee range is also calculated or justified using numerical vales from these simulations.

These equations are solved using a constraint equation at the point of contact of the stator and rotor(velocity is same)

$$l_p \frac{d\phi_S}{dt} = R\frac{d\theta_R}{dt} \tag{4}$$

Further the Torque generated by the steric is defined as follows,

$$\tau = -\frac{\partial V_{RS}}{\partial \theta_R}$$
$$\Rightarrow \frac{\partial V_{RS}}{\partial \phi_S} = \frac{\tau}{R} l_p$$

And, the torque from Proline hinge /conformation change is given by $F_p l_p$.

4 RESULTS AND DISCUSSION

The results from numerical simulation for deterministic model using different simulation methods are given in Figure 8

The curves are mostly linear because we did the simulation for the mechanical properly the chemical part is to be done by implementing a model for T_w(refer APPENDIX). The Euler method and ODE23 show a deviation from straight line , this might be due to the truncation error. But if we see properly even in ODE45 the curve is not perfectly linear, meaning the plot has a tendency to curve around a particular region.This region is can be called as the Knee speed region.From the Data this region occurs for loads around $0.1 < \zeta_L < 0.25$.

The values for T_m calculation is shown in figure 7. Here according to the paper the high loads has T_m approximately equal to 0.002 s. In figure 6 we can see the θ_R and ϕ_S value . Here we only restricted the θ_R value, but we can see that the ϕ_S reaches 40°. This is because during a single step there are two power stroke and the equations used are to model single loop of the stator. This means during the first half the equations model loop 1 and during the second half they model loop 3. This is possible because of the sign conventions we chose during the implementation. Hence the stator rotates in the same direction during both the power stroke . Hence we get added up ϕ_S value (instead of 20°).

Load (ZL) - Drag co-eff	Theta (rotor)	Phi (stator)
0.0050	0.238524092788252	0.681497407966433
0.6711	0.238533158340005	0.681523309542871
1.3372	0.239894495696686	0.685412844847672
2.0033	0.240218017956202	0.686337194160578
2.6694	0.241114910035143	0.688899742957551
3.3356	0.240890215779858	0.688257759371022
4.00167	0.241609949039934	0.690314140114097
4.6678	0.241094801685585	0.688842290530241
5.33389	0.241609550855826	0.690313002445217
6	0.241562947413302	0.690179849752291

Figure 6: simulated values for angles at the end of T_m

Load (ZL) - Drag co-eff	Theta (rotor)	Phi (stator)	Tm (s)
10	0.241324443513465	0.689498410038473	0.001951916398 97560 = 0.0020

Figure 7: T_m vale at high load

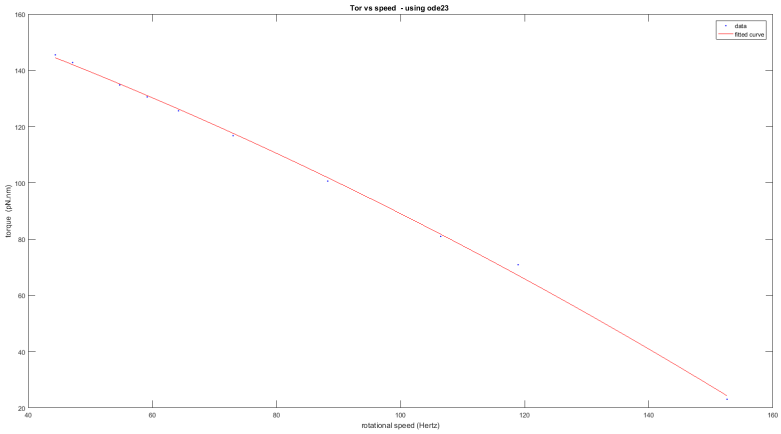

(a) using ODE23

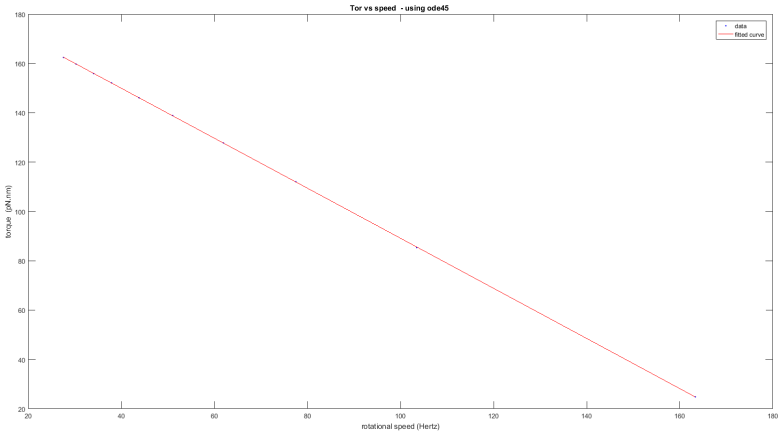

(b) using ODE45

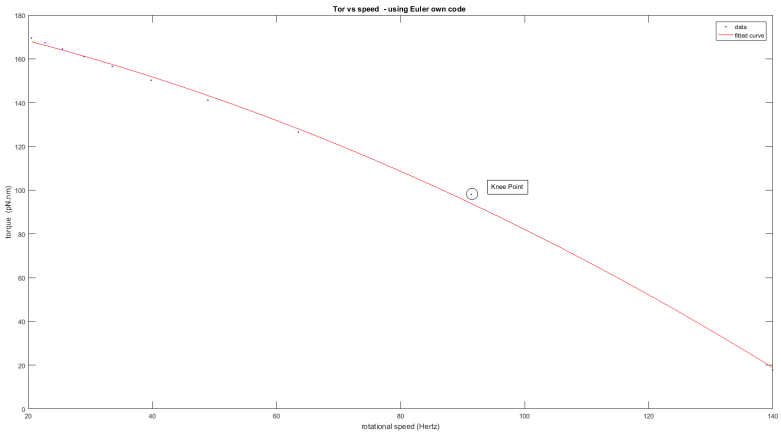

(c) using own code for forward Euler method implementation

Figure 8: Results from different ode simulators

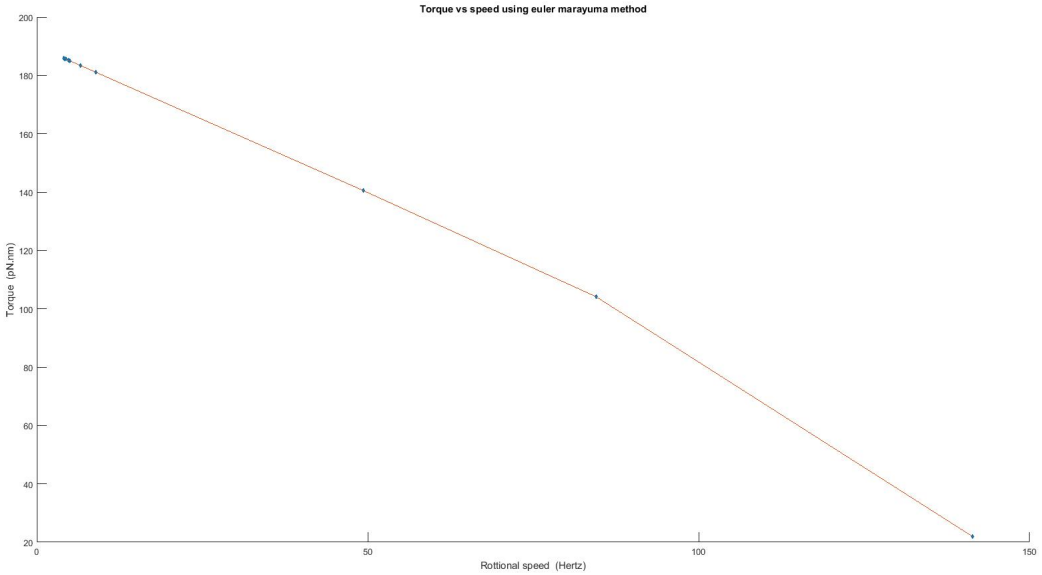

Figure 9: Results from SDE numerical simulation using Euler Maruyama method

The figure 9 shows the curve for the numerically simulated stochastic model,(note that we are still using average T_w value. This simulation was done for multiple number of steps and the cumulative average of τ was considered by keeping a threshold of 10^{-4}. Each mechanical step had 3000 time steps with each step=4.67×10^{-5}s.

(ZL) Loads	Tm values (secs)
0.0050	2.500e-05
0.6711	0.0002125
1.33722	0.0004
2.0033	0.000575
2.6694	0.0007625
3.3356	0.0009375
4.00167	0.001125
4.6678	0.0013
5.33389	0.0014875
6	0.0016625

(a) Numerical simulation for deterministic model

Load at knee point	Tm value (s)
0.2	2.7300000e-04

(b) numerical simulation for SDE model

Figure 10: These are the T_m values which is nearly equal to T_w values (points in the knee region)

As we mentioned before the nature of the curve depends on the T_w and T_m values . If $T_m > T_w$ then we end up in the plateau region (mechanically limited regime) and when $T_w > T_m$, then we would be in the downward curve or the linear region of the curve (

kinetically limited regime). This indirectly implies that the knee region is supposed occur at a load where the $T_m \approx T_w$. This idea is proved or justified from the numerical simulations . As we can see in the figure 10 for both deterministic and SDE model the knee region occurs at the above mentioned condition. This result also tells that the knee point observed in ODE23 , Euler method is actually a point belonging to the knee region as their T_m value is approximately equal to the T_w[8].

5 CONCLUSION AND FURTHER DEVELOPMENT

From the simulation and the analytical solution we were able to make a plot for the Torque vs speed. Even though we were not able to generate the desired shape, we almost got the curve for using an average T_w value from the paper. Tm calculation was validated with the paper and the knee point' nature has been explored both by numerically as well as theoretically. Implementation of Euler Maruyama for simulating SDE has been completed and desired results have been obtained.
FUTURE WORK: The future work for this model would be further implementation of the model

- $T_w$modelling was not implemented due to lack of experimental data. Data like ion concentration, dissociation constant, association constant. As of now from the 2013 paper these experimental data for Na^+ driven motor is present but, a theoretical model for connecting SMF,K_a,K_d,k_{on},k_{off},and maybe a term for the load size (like probability ,as at high loads probability of ion binding is less than in the low loads).
- To check whether the explicit inclusion of the probability term is required or implicitly this has been included while we are doing the time averaging of torque for a particular load.
- inclusion electrostatic potential term. This can be achieved by considering them as a dipole and energy can be modelled for different ϕ_S and θ_R values and can be used for numerical simulation.
- To create an ising model for seeing the back stepping of the motor as it is mentioned in the paper that due to normal thermal fluctuation the state of FliG can be changed and hence making it to go near the 2^{nd} and 4^{th} loop of MotA protein.
- Try get a more theoretical or give an explanation through the equations to explain the concave down curve instead of giving a vague explanation like domination between T_w and T_M to govern the morphology of the curve.
- Try to answer why different ODE solver gave different curve. Try to check T_m values for a different values of parameters and for different ODE solver. Try to implement RK_2 SDE solving algorithm and compare the studies.

6 APPENDIX

This section is to give some mathematical insight to the equations we are trying to solve. Now starting with those primary equations .

$$\zeta_S \frac{d\phi_S}{dt} = -\frac{\partial G(\phi_S, j)}{\phi_S} - \frac{\partial V_{RS}}{\partial \phi_S} - \frac{\partial \psi}{\partial \phi_S} + \sqrt{2k_B T \zeta_S} f_n(t)$$

$$\zeta_R \frac{d\theta_R}{dt} = -\frac{\partial V_{RS}}{\partial \theta_R} - \frac{\partial \psi}{\partial \theta_R} - k(\theta_R - \theta_L) + \sqrt{2k_B T \zeta_R} f_n(t)$$

$$\zeta_L \frac{d\theta_L}{dt} = k(\theta_R - \theta_L) + \sqrt{2k_B T \zeta_L} f_n(t)$$

These are the equations used for SDE modelling for the torque generation. The explanation of these terms are given in the METHODS section. Now let us create a deterministic model by avoiding or time averaging for a small time to avoid the noise term and the τ can still be considered as instantaneous as we are not necessarily averaging it till T_m just a short amount of time so that we could assume to neglect the noise term .Hence the equations are as follows. (as the model is for single stator we'll assume N=1,i denotes the number of the stator on which calculation is done)

$$N\zeta_S \frac{d\phi_S^i}{dt} = NF_p l_p - \frac{\tau}{R} l_p$$

$$\zeta_R \frac{d\theta_R}{dt} = \tau - k(\theta_R - \theta_L)$$

$$\zeta_L \frac{d\theta_L}{dt} = k(\theta_R - \theta_L)$$

These are the deterministic equation I'm gonna work with. As we can see $\phi_S, \theta_R, \theta_L, \tau$ 4 unknowns and 3 equations are there. Hence we use the help of a constraint equation (equation 4).

$$lp \frac{d\phi_S}{dt} = R \frac{d\theta_R}{dt}$$

Now we can algebraically solve the equations for $\frac{d\phi_S}{dt}, \frac{d\theta_R}{dt}, \frac{d\theta_L}{dt}, \tau$ variables so that we get equations in terms of $(\theta_R - \theta_L)$. Further we can subtract the equation for $\frac{d\theta_L}{dt}$ from the equation of $\frac{d\theta_R}{dt}$ so that finally we get an equation where in LHS we have $\frac{d(\theta_R - \theta_L)}{dt}$ and RHS has $(\theta_R - \theta_L)$ as the only variable so that we could integrate it and get the time dependent function for $\theta_R - \theta_L$.

$$\frac{d\phi_s}{dt} = -\frac{l_p(-F_p N R^2 + k(\theta_R - \theta_L)R)}{N\zeta_S R^2 + \zeta_R l_p^2}$$

$$\frac{d\theta_R}{dt} = -\frac{(kl_p^2(\theta_R - \theta_L) - F_p N R l_p^2)}{N\zeta_S R^2 + \zeta_R l_p^2}$$

$$\frac{d\theta_L}{dt} = \frac{k(\theta_R - \theta_L)}{\zeta_L}$$

$$\tau = NR\frac{F_p \zeta_R l_p^2 + Rk(\theta_R - \theta_L)\zeta_S)}{N\zeta_S R^2 + \zeta_R l_p^2}$$

The analytical solution for $(\theta_R - \theta_L)$ is,

$$(\theta_R - \theta_L)(t) = \frac{A(1 - e^{(-Bt)})}{B} \tag{5}$$

where $A = \frac{F_p N R l_p^2}{(N\zeta_S R^2 + \zeta_R l_p^2)}$, and $B = k[\frac{l_p^2}{(N\zeta_S R^2 + \zeta_R l_p^2)} + \frac{1}{\zeta_L}]$

To get a feel for ζ load let us write B as $\alpha + \frac{k}{\zeta_L}$. This implies $\alpha = k\frac{l_p^2}{(N\zeta_S R^2 + \zeta_R l_p^2)}$.

$$(\theta_R - \theta_L)(t) = \frac{A(1 - e^{(-(\alpha + \frac{k}{\zeta_L})t)})}{(\alpha + \frac{k}{\zeta_L})}$$

Now substituting in τ equation we get an expression for τ as a function of bot t and ζ.

$$\tau = NR\frac{F_p\zeta_R l_p^2 + Rk[\frac{A(1-e^{(-(\alpha+\frac{k}{\zeta_L})t)}}{(\alpha+\frac{k}{\zeta_L})})]\zeta_S)}{N\zeta_S R^2 + \zeta_R l_p^2}$$

Similarly, we can get an expression for ω_R,

$$\frac{d\theta_R}{dt} = \omega_R = -\frac{(kl_p^2[\frac{A(1-e^{(-(\alpha+\frac{k}{\zeta_L})t)}}{(\alpha+\frac{k}{\zeta_L})})] - F_p N R l_p^2)}{N\zeta_S R^2 + \zeta_R l_p^2}$$

We can see from both of these equations that the torque vs speed curve would be a straight line . Hence these equations only give the slope of the curve or the approximate values for the points to lie in a particular range of values(τ- max till 200pNnm and ω_R-max till 250 Hertz- for a single stator).This tells that by doing that time average over T_m and T_w gives the characteristic curve.

$$\tau_a vg = \frac{1}{(T_m + T_w)}\int_0^{T_m} NR\frac{F_p\zeta_R l_p^2 + Rk[\frac{A(1-e^{(-(\alpha+\frac{k}{\zeta_L})t)}}{(\alpha+\frac{k}{\zeta_L})})]\zeta_S)}{N\zeta_S R^2 + \zeta_R l_p^2}$$

And T_m calculation is nothing checking when θ_r goes to zero. This requires integration of ω_R from 0 to $T_m$such that θ_R goes from 0 to $\frac{2\pi}{26}$

$$\Rightarrow \frac{2\pi}{26} = \int_0^{T_m} -\frac{(kl_p^2[\frac{A(1-e^{(-(\alpha+\frac{k}{\zeta_L})t)}}{(\alpha+\frac{k}{\zeta_L})})] - F_p N R l_p^2)}{N\zeta_S R^2 + \zeta_R l_p^2}$$

And the average speed would be

$$\omega_{R_{avg}} = \frac{\frac{2\pi}{26}}{(T_m + T_w)}$$

From equation we might be able to tell how T_m depends on ζ_L. But as we can see its a complex or a bulky equation hence we prefer numerical simulations to ease our work. But doing this this analytical calculation gave us an insight about the curve and how those two time values govern the morphology. We cant just put numbers for these time values to achieve the curve as some detailed analysis/ proper model is required to give the meaning for the curve. Like how we have an expression for T_m, we need to create a proper model and have a similar one for the T_w.

SDE simulation: One other thing I learned for this project is "How to perform

SDE numerical simulations". The Brownian motion part of the equation (Thermal fluctuation) follows a different kind of integration process.

$$thermal fluctuation = \sqrt{2k_B T\zeta} f_n(t)$$

In this equation $f_n(t)$ is known as Wiener Process. Giving this name means that particular function follows some rules , which are

- $W_0 = 0$,
- W has independent increments : the future increments are independent of the past values - Markov process
- For $0 \leq s < t \leq T$, the random variable given by W(t)-W(s) is normally distributed with $\mu = 0$ and $\sigma^2 = t - s$, W(t)-W(s) $\sqrt{t-s}N(0,1)$, $N(0,1)$ is normally distributed variable with mean=0 and variance=1.

The integration of this Ito calculus, where there is an explanation for $dW^2 = dt$. When solving an equation with this process numerically , $W(t)dt = dW$ hence finally there will be a term with dt and one term dW. The dW(t) is implemented or substituted with $\sqrt{dt}N(0,1)$ for each time step[3].

$$X_{t_{i+1}} = X_{t_i} + \sum_{i=0}^{n} f(X_{t_i})(t_{i+1} - t_i) + \sum_{i=0}^{n} g(X_{t_i})\sqrt{(t_{i+1} - t_i)}N(0,1)$$

The above mentioned equation is called Euler Maruyama method for SDE calculation. Here Ito calculus is been implemented in forward Euler method.

ACKNOWLEDGEMENT

I'd like to Thank Prof. Manoj Varma from Centre for Nano Science and Engineering (CENSE) at Indian Institute of Science, Bangalore. I'd also like to thank the Division of Interdisciplinary Research, Dr. Anita and Animesh Mukherjee, and BSSE, Indian Institute of Science for the financial assistance and support. Finally I'd like to thank the whole BSSE department for organizing an amazing summer internship program, where I learnt a lot about Biology and How Engineering is used in this field through some lectures conducted by the "BEST" internship program.

References

[1] Howard C Berg and Linda Turner. Torque generated by the flagellar motor of escherichia coli. *Biophysical journal*, 65(5):2201–2216, 1993.

[2] Richard M Berry and Howard C Berg. Absence of a barrier to backwards rotation of the bacterial flagellar motor demonstrated with optical tweezers. *Proceedings of the National Academy of Sciences*, 94(26):14433–14437, 1997.

[3] Desmond J Higham. An algorithmic introduction to numerical simulation of stochastic differential equations. *SIAM review*, 43(3):525–546, 2001.

[4] Pushkar P Lele, Basarab G Hosu, and Howard C Berg. Dynamics of mechanosensing in the bacterial flagellar motor. *Proceedings of the National Academy of Sciences*, 110(29):11839–11844, 2013.

[5] Chien-Jung Lo, Yoshiyuki Sowa, Teuta Pilizota, and Richard M Berry. Mechanism and kinetics of a sodium-driven bacterial flagellar motor. *Proceedings of the National Academy of Sciences*, 110(28):E2544–E2551, 2013.

[6] Kranthi K Mandadapu, Jasmine A Nirody, Richard M Berry, and George Oster. Mechanics of torque generation in the bacterial flagellar motor. *Proceedings of the National Academy of Sciences*, 112(32):E4381–E4389, 2015.

[7] Michael D Manson, Pat Tedesco, Howard C Berg, Franklin M Harold, and Chris Van der Drift. A protonmotive force drives bacterial flagella. *Proceedings of the National Academy of Sciences*, 74(7):3060–3064, 1977.

[8] Giovanni Meacci and Yuhai Tu. Dynamics of the bacterial flagellar motor with multiple stators. *Proceedings of the National Academy of Sciences*, 106(10):3746–3751, 2009.

[9] Jasmine A Nirody, Yi-Ren Sun, and Chien-Jung Lo. The biophysicist's guide to the bacterial flagellar motor. *Advances in Physics: X*, 2(2):324–343, 2017.

[10] Edward M Purcell. Life at low reynolds number. *American journal of physics*, 45(1):3–11, 1977.

[11] Stuart W Reid, Mark C Leake, Jennifer H Chandler, Chien-Jung Lo, Judith P Armitage, and Richard M Berry. The maximum number of torque-generating units in the flagellar motor of escherichia coli is at least 11. *Proceedings of the National Academy of Sciences*, 103(21):8066–8071, 2006.

[12] Michael Silverman and Melvin Simon. Flagellar rotation and the mechanism of bacterial motility. *Nature*, 249(5452):73, 1974.

[13] Yoshiyuki Sowa and Richard M Berry. Bacterial flagellar motor. *Quarterly reviews of biophysics*, 41(2):103–132, 2008.

[14] Jianhua Xing, Fan Bai, Richard Berry, and George Oster. Torque–speed relationship of the bacterial flagellar motor. *Proceedings of the National Academy of Sciences*, 103(5):1260–1265, 2006.

[15] Junhua Yuan and Howard C Berg. Resurrection of the flagellar rotary motor near zero load. *Proceedings of the National Academy of Sciences*, 105(4):1182–1185, 2008.